Laboratório de Modelagem, Análise e Controle de Sistemas Não-Lineares

Departamento de Engenharia Eletrônica

Universidade Federal de Minas Gerais

Av. Antônio Carlos 6627, 31270-901 Belo Horizonte, MG Brasil

Fone: +55 3499-4866 - Fax: +55 3499-4850

Sensor Fusion for Irregularly Sampled Systems

Taiguara Melo Tupinambás

Dissertação submetida à banca examinadora designada pelo Colegiado do Programa de Pós-Graduação em Engenharia Elétrica da Universidade Federal de Minas Gerais, como parte dos requisitos necessários à obtenção do grau de Mestre em Engenharia Elétrica.

Orientadores: Prof. Bruno Otávio Soares Teixeira, Dr.
Prof. Leonardo Antônio Borges Tôrres, Dr.

Belo Horizonte, Maio de 2018

Contents

Todo list

Chapter 1

Introduction

1.1 Motivation

In nature it is possible to observe data fusion in a variety of phenomena. Animals combine signals from different senses, such as sight, hearing, smell, taste and touch, to recognize the surroundings. Plants have analogous mechanisms, which are used to modulate water consumption, to change the color of its leaves or to bend its structure towards the light, for instance. Throughout history, the sensory systems in living beings have evolved to assimilate multiple information coming from numerous sources in a highly complex and efficient way, in order to have a better perception of the environment.

Nowadays information fusion is studied in many fields of science, as a way of exploiting data from multiple sources to achieve better outcomes in comparison to those obtained if any of the sources were used separately (Dasarathy, 2001). Other terms have been used to denote the synthesis of information in technical literature, for instance, data fusion, sensor fusion, multi-sensor fusion or multi-sensor integration. To avoid confusion, the terminology used by (Elmenreich, 2002) will be adopted, whereby information fusion is understood as the overall term and sensor fusion is used in cases for which the sources of information are sensors.

Some research fields have been increasingly exploiting the advantages of sensor fusion techniques, such as robotics, military, biometrics and image processing. The main benefits expected are related to accuracy, due to the use of redundant or complimentary data, to dimensionality, that is additional information being created by a group of data, and to robustness against failure and interference. Consequently much effort has been put into the development and investigation of data fusion techniques. The work of (Khaleghi et al., 2013) presents an extensive review of different approaches available, categorizing them by the way sensor data uncertainty is represented, namely, probabilistic fusion, evidential belief reasoning, fuzzy reasoning, possibilistic fusion,

rough set-based fusion and hybrid fusion.

Data fusion techniques based on probability theory are the earliest available and perhaps the most popular until now. They are concerned with estimating the probability distribution functions (PDF) of the system states by means of the Bayesian approach. If the system is linear and Gaussian, then the Kalman filter (KF) guarantees optimal estimation. For nonlinear processes, KF generalizations were proposed, such as the extended Kalman filter (EKF) or the unscented Kalman filter (UKF) (Julier and Uhlmann, 2004). On the other hand, particle filters (PF) can be used to deal with both nonlinearities in the dynamics and non-Gaussian distributions (Arulampalam et al., 2002).

The most common class of systems studied in state estimation is the class of sampled-data systems, due to the wide use of digital devices. Although often described by continuous time differential equations, they can be modeled using discrete state equations, using approximation techniques (Phillips and Nagle, 1995). Usually the sampling period of such systems are constant and known. In other words, the sensors are considered to transmit data at regular intervals. However, for many applications, such assumption is not valid. The use of several redundant sensors, for example, with different sampling rates or unsynchronized with one another, leads to data being received at irregular instants. Additionally, when data from multiple sensors are transmitted through several subsystems in a network, there might be loss of packets and delays (Schenato et al., 2007) or even multiple information arriving simultaneously (Moayedi et al., 2011). In networked control systems, event-triggered sampling schemes have been proposed to optimize the access to communication channels (Hu et al., 2017), which will also generate time-varying sampling intervals. Nowadays, because of the ever-growing scientific advances, the technology of microprocessors, sensors and communication has become increasingly accessible, which continues to ensure that multiple sensor networks are more and more common.

Thus, despite improving accuracy and robustness of the estimation process, the fusion of data from multiple sensors might introduce challenges to the state estimation algorithms, due to sampling irregularities. Depending on how they take place, modifications to the KF and its generalizations can be carried out to tackle these abnormalities. In the work of (Fatehi and Huang, 2017), a fusion KF is proposed to estimate the states of a system with multi-rate measurements, whereby one of them is fast, regular and delay-free and the other is slow, irregular and randomly delayed. One application

of such system is for industrial process control, where there is online instrumentation characterized by the former and data from laboratory analysis, which are much more accurate. For a more general case, when the random delays are unknown, the work of (Gopalakrishnan et al., 2010) presents a critical analysis of the available methods for data fusion. They are separated into two categories: those that incorporate the delayed measurements upon arrival, and methods that rely in state augmentation, in order to assimilate the delayed information between estimation steps.

In general the proposed methods and their performance will depend on particularities of the sampling irregularities and how they are modeled. Time delays can be multiples of a base sampling period, for instance. In those cases, delays can happen at single or multiple lags (Peñarrocha et al., 2012), can lead to out-of-sequence measurements (Anxi et al., 2005; Westenberger et al., 2013) or there can also be data dropout (Zhu et al., 2013). Nevertheless, the system can be described by a time-invariant discrete state equation, but with a particular representation of the measurement model. When the instants take place after random time intervals, the discrete-state representation leads to a time-varying system, since the sampling period changes over time. Some researches treat the variable measurement instants as stochastic processes (Micheli and Jordan, 2002) or as a periodic sampling interval subject to noisy perturbations (Shen et al., 2016). Generally, the instant is considered to be known and the methods assimilate such information in the algorithm.

To the best of the author's knowledge, no method was proposed so far to take the irregularity into account and improve the estimation efficiency, for the cases in which the random time instant the signal was measured is not known or not reliable. If the sampling irregularity is caused due to the lack of sensor synchronization in the network, several algorithms can ensure a common timescale (Sivrikaya and Yener, 2004), at the expense of additional investments or energy use. Another approach, believed to be largely used on practice, is to disregard the irregularities, assimilating the measurements once they arrive, *FALTA REFERÊNCIA (dificuldade em encontrar)*. In this case, additional noises are tuned in the estimation process, but it might be irrelevant to the overall performance.

Knowing to what extent the estimation accuracy is deteriorated by ignoring the additional uncertainty caused by the sampling irregularity is important to decide whether or not to invest in synchronization. In addition, the investment in more sensors to the network in order to improve accuracy might not pay off, if it increases the occurrence

of irregularities. However there are no detailed studies on the behavior of the degradation in accuracy due to not addressing properly the irregularity in the sampling process. Therefore, this work assesses the differences in state estimation performance for systems with random sampling intervals with and without timestamp for different scenarios. The purpose is to shed some light on the trade-off for investments in sensor networks and synchronization.

1.2 Problem Formulation

Consider the stochastic nonlinear sampled system

$$\dot{x}(t) = f(x(t),u(t),w(t),t), \tag{1.1}$$

$$y(t_k) = g(x(t_k - \delta_{t_k}),v(t_k),t_k), \tag{1.2}$$

where f: $\mathbb{R}^n \times \mathbb{R}^p \times \mathbb{R}^q \times \mathbb{R}^+ \rightarrow \mathbb{R}^n$ and g: $\mathbb{R}^n \times \mathbb{R}^r \times \mathbb{R}^+ \rightarrow \mathbb{R}^m$ are, respectively, the process and observation models, assumedly known. We assume that for all $k \geq 1$, the observations $y(t_k) \in \mathbb{R}^m$ and the first two moments of the random variables x_0 and $v(t_k)$ are known, where $x_0 \in \mathbb{R}^n$ is the initial state vector and $v(t_k) \in \mathbb{R}^r$ is the observation noise. Observations are taken at random time instants t_k and are considered to be sorted ($t_{k+1} > t_k, \forall k \in \mathbb{N}^+$) and defined by the time intervals $h_0 \triangleq t_1$, $h_k \triangleq t_k - t_{k-1}$, $\forall k \geq 1$. In this work, we assume that the observation time instants t_k are given by a Poisson random process. That is, the time intervals h are independent and identically distributed exponential random variables with a known parameter λ_h, that is $h_k \sim \mathcal{E}(\lambda_h)$, where $\mathcal{E}(\lambda)$ defines an exponential PDF, with parameter λ, which is also its expected value. An example of time intervals produced by such a random process is illustrated in Figure 1.1.

This sampling model characterizes a common application for an event-based sampling scheme or for a networked control system with unsynchronized sensors. (Micheli and Jordan, 2002), for instance, considers a set of N identical sensors measuring the state variables of a physical process every L seconds. They prove that, if the sensors are independent and unsynchronized and N is big enough, the waiting time between the realization of two consecutive measurements can be approximated by an exponential random variable $\mathcal{E}(\lambda)$, where the parameter is given by $\lambda = N/L$.

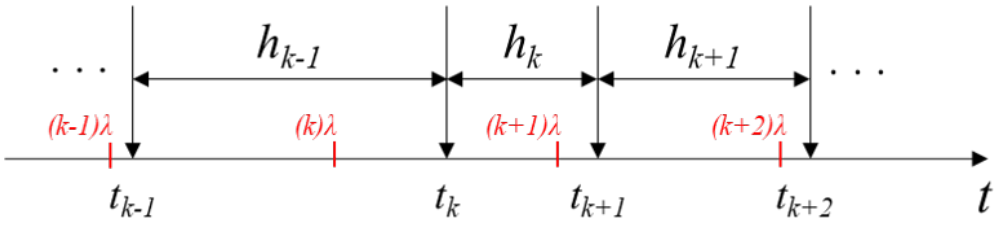

Figure 1.1: Irregular sampling process modeled by a Poisson random process. Regularly spaced time intervals λ are shown in red. An example of time instants t_k realization is also shown, with the respective random time intervals h_k. The expected value of time interval is given by $E(h_k) = \lambda$.

Arrival times to the estimator may be delayed during transmission by a random time amount δ_t, also given by exponential random variables, with parameter λ_{δ_t}, according to Figure 1.2. Out-of-sequence measurements (OOSM) are not considered in this work. We assume that, in case a delayed measurement is to arrive later than future measurements, it gets lost in transmission.

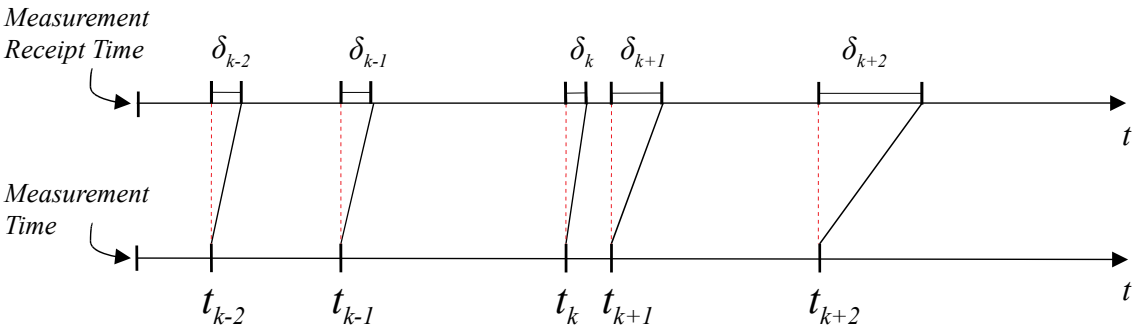

Figure 1.2: Randomly delayed measurements, modeled as exponential random variables. Random measurement times t_k are received by the estimator after a random delay δ_{t_k}

Input data $u(t)$ are available at regularly spaced intervals T, that is $u(iT) \in \mathbb{R}^p$, $\forall i \geq 1$ are known. $w(t) \in \mathbb{R}^q$ is process noise.

When time-stamp information is available, data assimilation can be performed at the correct measurement instants t_k. When they are not, the assimilation moment is considered to be the random receipt time instant or the next estimation moment, when there are no transmission time delays.

We wish to estimate the state vector $x(t)$ and its covariance recursively, at regularly spaced time intervals T, given their initial values (x_0, P_0), the process model (1.1), the input or control signals $(u(t) : t \leq kT)$ and the set of past observations $y(t_k) : t_k - \delta_{t_k} \leq kT$. The knowledge of the time intervals $h_{k-1} : t_k - \delta_{t_k} \leq kT$ is also taken into consideration when time-stamp information is available. We assume that the average time interval of observations λ_h is greater than or equal to T by a factor $\alpha \geq 1$, i.e. $\lambda_h = \alpha T$.

1.3 Objectives

1 frase para o objetivo geral Objetivos específicos

1.4 Text Outline

Chapter 2

Irregular Sampling

In this chapter, we review the irregular sampling problem. First, in Section 2.1 we categorize the different types of irregularities that may occur in sampling and discuss the main causes and its particularities. A diagram is built by categorizing the main types studied in the scientific literature.

2.1 Introduction

Sampling irregularities may occur due to a variety of issues, sometimes as undesired side effects of using large sensor networks architectures and others due to deliberate non-uniform sampling schemes. In this section we try to categorize and review the main irregularities observed in practice. The diagram in Figure 2.1 provides a simplified overview of them, separated by their sources.

Networked system monitoring and control appears to be the main cause of irregular sampling. Unreliable communication channels may lead to random time delays and loss of information, specially if the data are transmitted using a common media (Sahebsara et al., 2007; Moayedi et al., 2011). In case they get randomly interrupted during transmission or if a sensor fails at some point, the signal received may predominantly contain noise, causing uncertain observation or packet dropouts (Hadidi and Schwartz, 1979; Wang et al., 2009). Systems that are observed by a large number of desynchronized sensors will provide observations at random time intervals (Micheli and Jordan, 2002). If they are synchronized but designed to operate in a centralized fashion, there is a chance that different time delays are produced due to distinct transmission routes for each sensor (Bar-Shalom, 2000; Challa et al., 2003; Anxi et al., 2005).

However the communication networks shall not always be held responsible. Some applications are designed to be measured in an irregular way. In event-based schemes, for example, the measurements are transmitted only when certain conditions are met

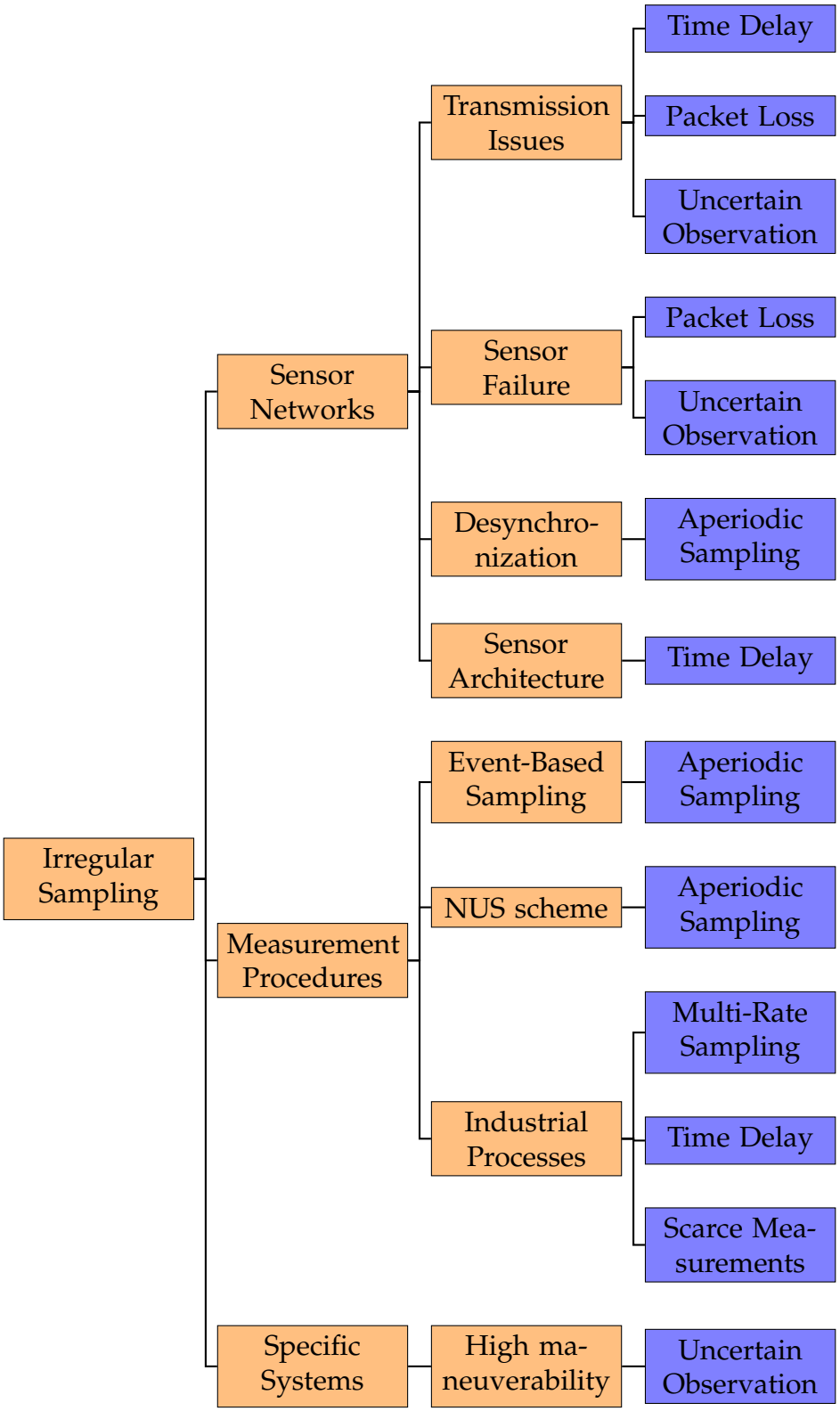

Figure 2.1: Irregular sampling diagram, showing the main causes (in orange) and effects (in blue) of irregularities

(Liu et al., 2014; Zou et al., 2017). Such approach can reduce communication resource consumption substantially (Hu et al., 2017), but will cause aperiodic sampling. Non-Uniform Sampling (NUS) is also intentionally used as an alias detection method (Kunoh, 2015) or to enhance the spectral resolution of signals, largely used in Nuclear Magnetic Resonance (NMR) spectroscopy analysis (Hyberts et al., 2013). In other situations, due to the nature of the process being observed, the measurement strategy relies on different procedures. A lot of chemical processes, for instance, can be measured in an online, fast rate and delay free fashion, but provides inaccurate data. Therefore, lab analyses are used to improve estimation quality, but they are usually gathered at slower rates, sometimes irregularly and with possible time delays (Fatehi and Huang, 2017). Other industrial applications suffer from the same dilemma, and the sampling scheme ends up with a multi-rate data transmission, with random time delays and possibly measurement scarcity (Peñarrocha et al., 2012).

Finally, sampling irregularities might also appear due to a specific nature of a system. In some high maneuverable target-tracking applications, for example, there is a chance that the sensor misses the target, transmitting only noise, leading to the so called uncertain observation issue (Wang et al., 2009; Chen et al., 2013).

On the next sections, we review the main irregular sampling effects.

2.2 Time Delay

Time-delay systems (TDS) are probably the most common mathematical representation to time delays in practice. The works of (Richard, 2003; Fridman, 2014) and the references therein provide a good coverage of the subject. In TDSs, there might be delays in the input or in the output signals, introduced by communication networks, or even in the states themselves. The latter phenomenon is called system with aftereffect or dead-time. Since we are studying the irregular sampling issue, only signal delays are relevant to us.

Considering delays in the measurement model only, (Lu et al., 2005) studied the estimation problem when they are constant and known. They describe a linear measurement model as

$$y_i(t) = H_i(t)x(t_i) + v_i(t) \tag{2.1}$$

where $i = 0, 1, \ldots, l$ and l is the number of different known delays. $y_i(t) \in \mathbb{R}^{p_i}$ are delayed measurements and $v_i(t) \in \mathbb{R}^{p_i}$ the measurement noises. The known delayed time instants are given by $t_i = t_{i-1} - d_i$, with $d_0 = 0$, $d_i > 0$ for $i > 0$ and $t_0 = t$.

If the delays are multiple of a constant value, observations might be received a burst, when more than one packet arrive between two consecutive sampling instants. In such situations, the estimator might use only the latest measurement and discard all others, or implement a buffer to iterate over all received packets, when burst arrivals happen (Moayedi et al., 2011).

However, in many applications the measurements are received by the estimator with irregular and unknown delays. In such cases, time delays can be interpreted as a stochastic process $d(k)$, varying randomly throughout time. (Han and Zhang, 2009) describes a discrete-time measurement model for random delayed observations as

$$y(k) = H(k)x(k - d(k)) + H(k)v(k) \tag{2.2}$$

where $d(k)$ is a random but bounded time delay, assumed to be a discrete-time Markov Chain observable at each sampling time k.

Multiple of a known lag or not, delayed measurements from a multisensor system are subject to arrive disordely, which leads to the sampling irregularity commonly known as to as out-of-sequence-measurements (OOSM). It can be classified in three ways, depending on the number of lags, according to Figure 2.2.

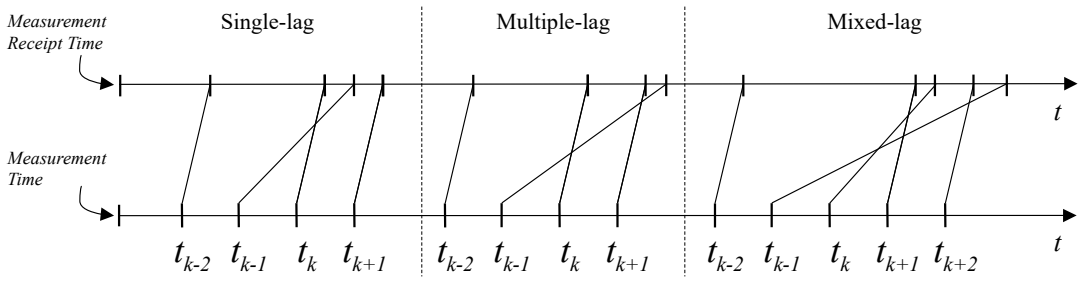

Figure 2.2: Different classes of out-of-sequence measurements irregularities

(Anxi et al., 2005) describes four different filtering approaches to deal with OOSM: reprocessing, that stores filter results to rollback with the time-delayed measurement; data buffering, that holds a set of measurements, greater than maximum expected lag,

to be sorted before filtering; discarding data, that neglects time-delayed measurements; and directly updating, that uses the delayed information to update current state estimate. (Bar-Shalom, 2000) used the last approach to describe an optimal filter for the single-lag case.

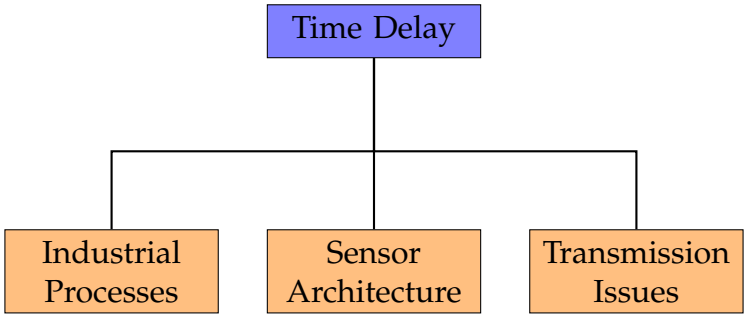

Figure 2.3: Irregular sampling diagram, showing the main causes (in orange) and effects (in blue) of irregularities

2.3 Packet Loss

When data are being transmitted by a large network of sensors, there is a probability they can get lost in the way or they might arrive after a significant delay, which is equivalent to a loss for practical applications (Sinopoli et al., 2004). Usually referred to as packet dropout/loss, missing or intermittent observations, they may happen due to node failures, network congestion, limited bandwidth or temporal failure.

Mathematical description of packet dropouts can be carried out recursively, as described in (Ma and Sun, 2011), by

$$\begin{aligned} z(t) &= H(t)x(t) + v(t), \\ y(t) &= \xi(t)z(t) + (1 - \xi(t))y(t-1), \end{aligned} \tag{2.3}$$

where $z(t) \in \mathbf{R}^m$ is the measured output transmitted to the estimator, $v(t) \in (R)^m$ is white noise, $y(t) \in \mathbf{R}^m$ is the measurement received by the estimator and $\xi(t) \sim Ber(p)$ is a Bernoulli random variable that takes the value 1 with probability p and 0 with probability $1-p$. That is, when $\xi(t)$ is 1, there is no packet dropout. If $\xi(t)$ is 0, however, the latest output is used at current time, in a recursive fashion.

Another way of describing multiple packet dropouts is by limiting the amount of consecutive dropouts (Shuli Sun et al., 2008), where the received measurements are defined by

$$\begin{aligned} y(t) =& \xi(t)z(t) + (1-\xi(t))\xi(t-1)z(t-1)+\dots \\ &+ (1-\xi(t))(1-\xi(t-1))\dots(1-\xi(t-N+1))z(t-N), N \geq 1, \end{aligned} \tag{2.4}$$

Such a model dictates that the measurement used by the estimator will be only the most recent available, and the amount of missing observations is limited to N. This conclusion can be drawn by the fact that

$$\xi(t) + (1-\xi(t))\xi(t-1)+\dots+(1-\xi(t))(1-\xi(t-1))\dots(1-\xi(t-N+1)) = 1. \tag{2.5}$$

2.4 Uncertain Observation

For some applications, there is a chance that the observation signal sent to the estimator contains only noise. According to (Jaffer and Gupta, 1971), it happens as a consequence of two situations: the observation was taken, but was lost during transmission, due to communication failures; or it was not transmitted at all, as it may happen for target tracking systems, for example, when the object being observed is not tracked at a sample time. An observation model for a sampled-data system can be described as

$$y(k) = \gamma(k)Cx(k) + Dv(k) \tag{2.6}$$

where $\gamma(k) \sim Ber(p(k))$ is a Bernoulli random variables, taking values of 0 or 1, with probabilities $p(k)$ and $1 - p(k)$, respectively.

Unlike the packet dropout problem, when the missing data are associated with the total absence of signal, the issue of uncertain observation has to be dealt with differently. A common approach is to detect the existence of signal prior to the assimilation, using a likelihood ratio test. (Middleton and Esposito, 1968) proposes a joint approach to systematically detect and extract information from observation signals. If the estimator and detector are developed separately, te probability of false alarms is not used in

the estimator, making it suboptimal. (Nahi, 1969) developed an optimal recursive estimator, that uses the information of the random variable γ in the algorithm, assuming it is independent and identically distributed. (Hadidi and Schwartz, 1979) generalized the work of Nahi, for the case when the uncertainty of the signals presence is described by a Markovian sequence of binary random variables.

2.5 Aperiodic Sampling

All irregularities discussed so far may be present even in a periodic sampling scheme. However, for some applications, the sampling intervals are time-varying due to a variety of phenomena, causing what is called as aperiodic or asynchronous sampling. It can be the case of networked and embedded control systems, with unpredictable networked-induced issues, like irregular faults on samplers, oscillated loads, intermittent saturation or even variations in system components or parameters (Shen et al., 2016). Some imperfections may cause what is known as sampling jitter noise, which leads to time intervals being almost uniform. Automotive applications, radar imaging or event controlled systems are a few examples. In them, jitter noise happens due to sampling frequency similar to clock frequency, sampling requests delayed by the network or imperfect synchronization (Eng and Gustafsson, 2005). For networks with a large amount of unsynchronized sensors, measurement arrival time intervals are randomly spaced and can be modeled as a stochastic process (Micheli and Jordan, 2002).

Sometimes, the system being observed has particularities that causes the aperiodic sampling. One example is seismology, where the spatial coordinates are irregularly sampled, because of natural obstacles (Marvasti, 2001). Other large scale systems, such as power grids, have sensors with a huge geographical separations, and different communication links to the estimation hub, which causes multiple and random inter-observation intervals (Yan et al., 2017).

Whereas for most cases, the non-uniformities in sampling time intervals appear as unwanted effects, there are cases when the sampling rule is designed to work irregularly. If there are limitations of communication resources (limited bandwidth or computation capacity) or a need for a reduced energy consumption, for example, time-driven sampling might be neglected in favor of an event-based scheme. In such strategy,

an event-triggering mechanism is responsible for determining the sampling instants, according to Figure 2.4. For time-driven schemes, a clock triggers the transmission instants (a), while event-driven sampling instants depends on the sensor output itself with an optional feedback loop from the estimator, to assess estimation performance. Therefore, the trigger mechanism design provides a trade-off between performance and resource consumption efficiency, attracting a lot of research interest (Liu et al., 2014). The most common strategy for event-driven state estimation is the send-on-delta (SOD) (Miskowicz, 2006), which triggers the transmission when the value of the measured state deviates from the previous assimilated observation by an interval $\pm\Delta$, with $\Delta > 0$. Other strategies were studied in (Zou et al., 2017). To avoid the risk of unexpected high amount of triggered measurements in a short period of time, which can lead to the dreaded Zeno behavior (Tabuada, 2007), lower-bounds can be defined both for the Δ value or for some explicit minimum inter-event time.

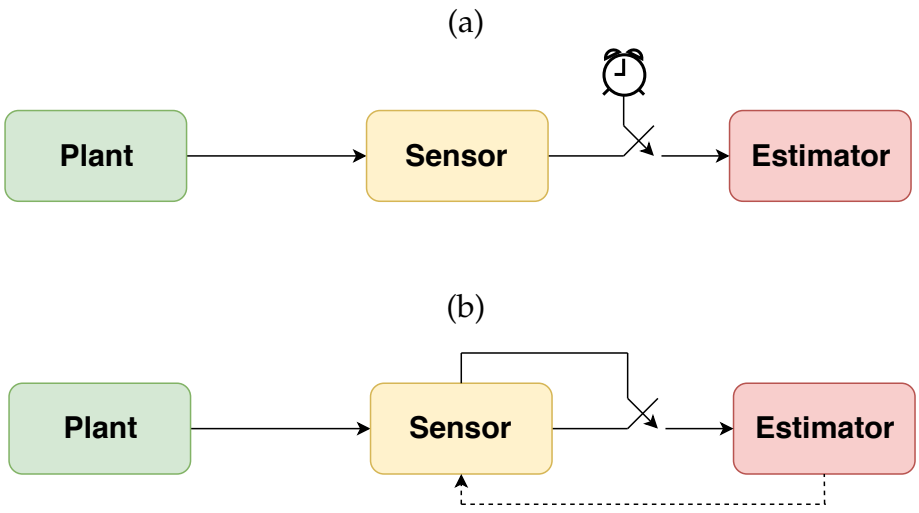

Figure 2.4: Time-driven (a) and event-driven (b) sampling schemes. The connection between sensor and estimator is triggered by different mechanisms.

Generalizations of aperiodic sampling can be divided in two categories, based on how the estimator perceives the irregularity: as time noise added to a periodic pattern; or as a stochastic process, according to Figure 2.5.

For the first case, the time interval δ_k can be defined as:

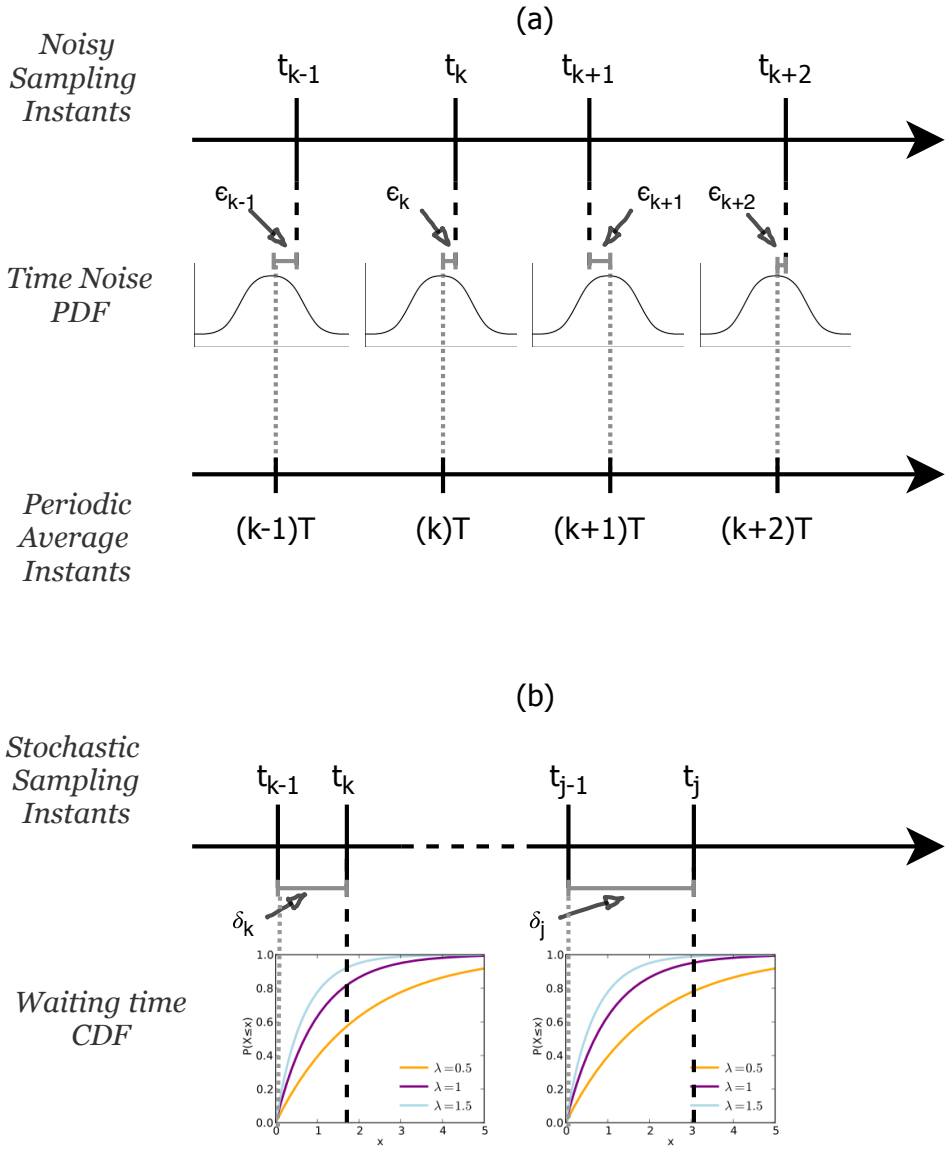

Figure 2.5: Aperiodic sampling categories: (a) noisy sampling over periodic intervals, with a Gaussian random variable added to expected time instants; and (b) sampling instants modeled as a stochastic process, with time intervals characterized by an exponential random variable (cumulative distribution functions are shown, for different λ parameter value.)

$$\begin{aligned} t_k &\triangleq kT + \epsilon_k, \\ \delta_k &\triangleq t_k - t_{k-1} \end{aligned} \tag{2.7}$$

where t_k is the kth sampling instant, T is the periodic time interval and ϵ_k is the deviation from the expected value kT. Note that, if the sampling time instants are a sequence of i.i.d Gaussian random variables, with variance σ^2, that is $t_k \sim \mathcal{N}(kT,\sigma^2)$, $\forall k \sim \mathbb{N}$, then the time interval random variable is Gaussian, with expected value T and variance $2\sigma^2$, that is $\delta_k \sim \mathcal{N}(T,2\sigma^2)$.

For the stochastic process generalization, time instants t_k can be modeled as ordered ($t_{k+1} > t_k$, $\forall k \sim \mathbb{N}$), and defined by time intervals δ_k, such as:

$$\begin{aligned} \delta_k &\triangleq t_k - t_{k-1}, \\ \delta_0 &\triangleq t_1 \end{aligned} \tag{2.8}$$

where time intervals are given by a probability density function, usually of exponential or Erlangen type (Kanchanaharuthai and Wongsaisuwan, 2002).

The measurement model of a linear system with aperiodic sampling can be modeled as

$$y(t_k) = H(t_k)x(t_k) + v(t_k) \tag{2.9}$$

where t_k are the sampling time instants and matrix $H(t_k)$ is time-varying, if derived from the discretization of a continuous time system.

2.6 Multi-Rate Sampling

The last irregularity discussed is the multi-rate sampling. Generally, it refers to multiple sensors measuring the same system at different sampling rates. Many industrial processes need to control challenging variables that can be measured by online instruments that provide regular, fast rate and delay free information, but with low precision. Therefore, more accurate data are needed and usually available after slow and irregular laboratory analysis (Peñarrocha et al., 2012; Fatehi and Huang, 2017). The combination of both sources of measurements leads to a multi-rate sampling scenario.

A more common approach is the use of various sensors measuring the same physical information, to obtain better estimates, which has been drawing attention from real world applications, such as target tracking, robotics, surveillance and military. For such strategy, the sampling rates perceived by the estimator are often different from

one another. The work of (Lin and Sun, 2016) and the references therein provide a wide coverage of scenarios derived from multi-sensor multi-rate systems.

Figure 2.6 illustrates the ways multi-rate sampling can manifest in a system. The different rates from the various sensor devices can be periodic (a), aperiodic (b) or even a mixture of both, as is the case for most industrial applications with laboratory analysis.

Aperiodic sampling rates can be described the same way as in Section 2.5, by equation **??**. Periodic multi-rate measurements can be modeled as

$$y_i(k_i) = H_i(x(k_i)) + v_i(k_1) \tag{2.10}$$

where $y_i(k_i)$ represents the k_i^{th} observation from sensor i and H_i is the discrete measurement model matrix.

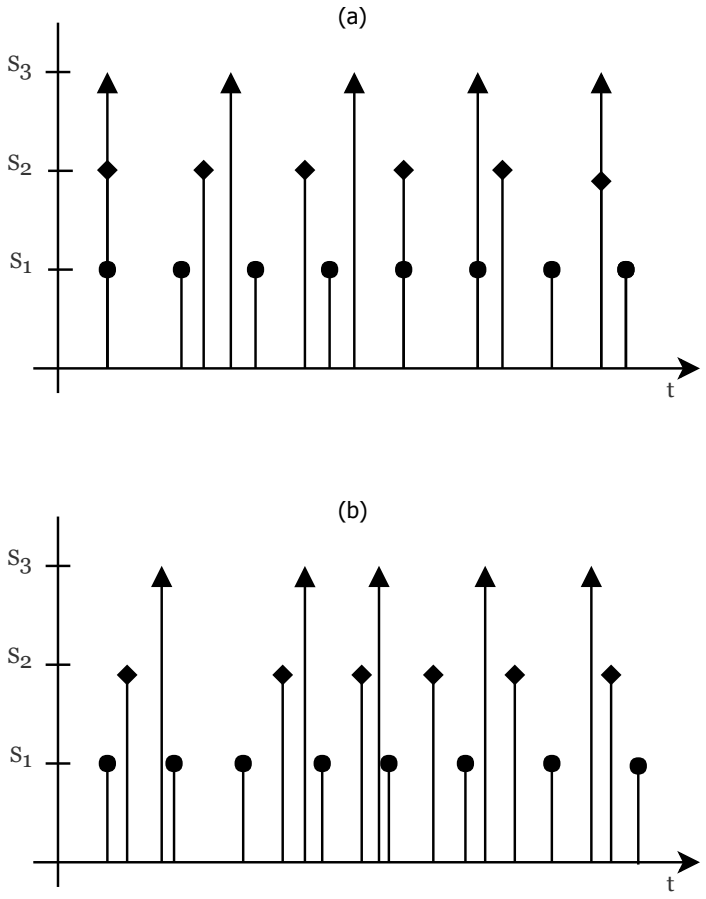

Figure 2.6: (a) Periodic multi-rate and (b) aperiodic sampling scheme.

Chapter 3

Sensor Fusion

In this chapter, we review sensor fusion techniques. We start with a brief explanation on the four different types: possibilistic, fuzzy reasoning, evidential belief e probabilistic. The latter is further explained, since it is the one used in the simulated examples. Specific techniques to deal with irregular sampling in sensor fusion are also addressed.

3.1 Introduction

Explicar brevemente sobre os tipos de fusão sensorial: possibilistic, fuzzy reasoning, evidential belief e probabilistic (Khaleghi et al., 2013). Focar no probabilistic.

3.2 Probabilistic Sensor Fusion

Entrar em maiores detalhes do probabilistic, explicando KF e o PF (caso seja utilizado no trabalho).

3.2.1 Kalman Filters

3.2.2 Particle Filters

3.3 Sensor Fusion Techniques

Para fusão de informações múltiplas de observações, explicar os quatro grandes grupos: parallel filter (multi-output system, multi-output KF), sequential filter (kfusing first output as the prediction for the secod output), outputs fusion (outputs are fused using the noise covariance) e track-to-track fusion (single-output KFs fused considering correlation). (Willner et al., 1976; Fatehi and Huang, 2017)

Tentar agrupar os principais métodos de filtragem, por tipo de irregularidade (possivelmente uma grande tabela)

Chapter 4

Simulation Methods and Assumptions

4.1 State Estimation with Irregular Sampling

Um esquemático ilustrativo é apresentado na Fig., onde $\alpha = 5$, i.e. a taxa média de amostragem das observações $1/\lambda$ é cinco vezes mais lenta que a frequência de amostragem $1/T$ dos sensores que disponibilizam informações de entrada. A cada T segundos, ou seja no intervalo de tempo entre dois instantes de amostragem das entradas pode haver ou não informações de observação. No cenário ilustrado pela letra **A** na Fig. 4.1, não há medições disponíveis. Durante o intervalo **B** há apenas uma medição, ao passo que em **C** há mais de uma observação disponível.

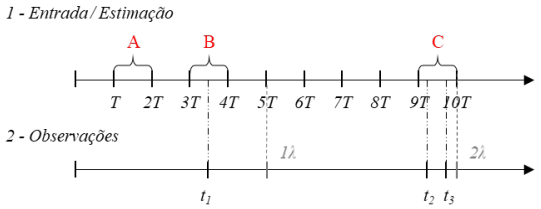

Figure 4.1: Exemplos de instantes de amostragem da entrada e das estimações (1) e das observações (2). Os instantes múltiplos de λ, igual ao intervalo médio de amostragem das observações são apresentados em cinza escuro, para referência.

4.1.1 Input Irregular Sampling

Em caso de amostragem irregular também na entrada, um esquemático dos instantes de estimação, amostragem e entrada pode ser observado na Fig. 4.2

Para atrasos de transmissão:

Nas próximas subseções é apresentado como os algoritmos de estimação tratam os cenários **A**, **B** e **C** para os casos em que o carimbo de tempo está e não está disponível.

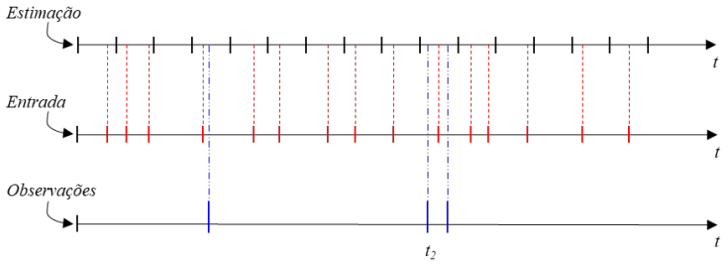

Figure 4.2: Exemplos de instantes de amostragem de estimação(1), da entrada (2) e das observações (3). Os instantes múltiplos de λ, igual ao intervalo médio de amostragem das observações são apresentados em cinza escuro, para referência.

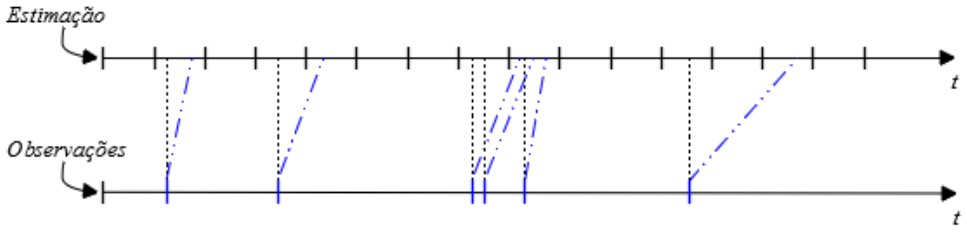

Figure 4.3: Exemplos de instantes de amostragem de estimação(1), da entrada (2) e das observações (3). Os instantes múltiplos de λ, igual ao intervalo médio de amostragem das observações são apresentados em cinza escuro, para referência.

4.2 With Timestamp

Sabendo o momento exato t_k em que as observações são medidas, é possível assimilá-las no instante correto, considerando intervalos de tempo variáveis para o algoritmo de filtragem. Para isso, o modelo matemático em () é discretizado a uma taxa δt_j^* variável. Para a simulação deste artigo, os valores de δt_j^* são calculados a partir da união de todos os instantes de tempo correspondentes às chegadas de sinais de entrada ou de medição em um único vetor, de forma ordenada. Por meio da subtração de dois instantes consecutivos, é possível obter os intervalos de tempo de integração δt_j^* correspondente. No caso de uma versão *online*, a integração das equações diferenciais é executada a medida que um sinal de entrada ou um sinal de medição de saída é recebido. Nesses momentos, são utilizados o intervalo de tempo entre o último sinal recebido e o instante atual. Além disso, quando o sinal recebido é um sinal de entrada, é executada apenas a etapa de predição. E, quando o sinal for de medição, acontecem as duas etapas de predição e assimilação de dados, considerado um segurador de

ordem zero para a entrada. O fluxograma da Fig. 4.4 representa o passo a passo desse algoritmo, apresentando as etapas executadas quando o sinal é de entrada ou de observação.

Dessa forma, no cenário **B** da Fig. 4.1, o algoritmo executa uma etapa completa de predição e assimilação de dados dos instantes $3T$ até t_1, considerando o intervalo $\delta t_4^* = t_1 - 3T$ (note que há 3 intervalos de tempo δt_j^*, antes o instante t_1). Em seguida é feita uma etapa de predição entre t_1 e $4T$. Durante o intervalo de tempo de integração entre t_1 e $4T$, considerou-se que a entrada permaneceu constante desde a sua última atualização em 3T. Ou seja, assume-se que não houve variação na entrada para essa etapa de predição. Caso mais de uma observação seja medida entre duas entradas (cenário **C**), são executadas etapas completas de filtragem para cada observação disponível e, ao final, uma etapa de predição entre a última observação e a próxima entrada.

4.3 Without Timestamp

Quando o carimbo de tempo está disponível, a assimilação de dados do algoritmo pode ser feita nos momentos exatos da medição. Para isso, a integração das equações diferenciais via discretização deve acontecer com intervalos de tempo variáveis, no caso deste trabalho utilizando o método de Runge-Kutta de 4ª ordem. Dessa forma, (1.1) pode ser reescrita como

$$x(t_j^*) = f_\mathrm{d}(x(t_{j-1}^*), u(t_{j-1}^*), w(t_{j-1}^*), t_{j-1}^*), \tag{4.1}$$

em que $t_j^* = t_{j-1}^* + \delta t_j^*$ e $t_0^* = 0$. Cada valor δt_j^* corresponde ao intervalo de tempo entre o último instante t_{j-1}^* em que se registrou a chegada de um sinal, seja ele de entrada ou de observação, e o próximo instante de tempo t_j^* em que um valor de entrada ou de observação é obtido, conforme será detalhado no Capítulo 4. Entre instantes de observação e de entrada é utilizado um segurador de ordem zero, considerando a ultima informação disponível.

Por outro lado, se o carimbo de tempo não é levado em conta, (1.1) pode ser reescrito como

$$x_n = f_\mathrm{d}^*(x_{n-1}, u_{n-1}, w_{n-1}, n), \tag{4.2}$$

em que $t = nT$.

Quando não há carimbo de tempo nas medições, o algoritmo de filtragem não sabe o momento exato da medição t_k. Assim, o instante de tempo considerado para a etapa de assimilação de dados é sempre o próximo instante múltiplo de T, i.e. quando a próxima informação de entrada está disponível. Existem apenas dois cenários de estimação nesse caso. Primeiro, quando não há medições disponíveis entre duas entradas, o estimador executa apenas a etapa de predição entre os intervalos de tempo iT e $(i+1)T$, conforme cenário **A** da Fig. 4.1. Segundo, nos casos representados pela letra **B**, o estimador considera que a observação foi feita no próximo instante multiplo de T em que há informações de entrada. No exemplo da Fig. 4.1, a medição feita no instante t_1 é assimilada no instante $4T$. Caso haja mais de uma observação entre duas entradas (cenário **C**), a mais antiga é descartada. Os passos de discretização do modelo utilizados pelo UKF são sempre $\delta t = T$, havendo ou não observações disponíveis.

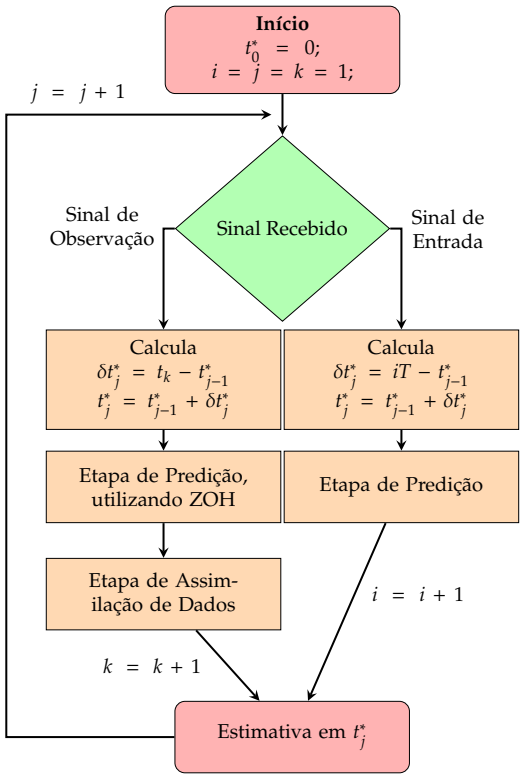

Figure 4.4: Diagrama ilustrativo da versão *online* do estimador que considera o carimbo de tempo. Os índices i, j e k representam, respectivamente os contadores dos sinais de entrada, estimação e da saída.

Chapter 5

Results

In this chapter, we present simulation results for two different systems: a linear system with two under damped modes and a nonholomonic unicycle position system.

REVISAR

We begin by describing the simulated systems as a state-space representation. First system is discretized and a discrete Kalman filter is used for the estimation of the unicycle position. The second one is represented as a continuous-time process model with digital measurements of one stby aate. We wish to estimated a all states sampled-data Kalman filter.

For both cases, we start evaluating the effect of time-stamp information in the estimation algorithm for three different irregular sampling scenarios, without time-delay in the observations: variation of the observation signal-to-noise ratio, variation of the observation average sampling rate, and variation of the relation between estimation regular sampling rate and output irregular average sampling rate.

Then we add random time-delay to the observation model and evaluate the effect for the same three scenarios plus a fourth one, where we vary the average time-delay.

5.1 Linear System

Descrever as motivações por trás do estudo do sistema linear: variáveis controladas, resultado esperado conhecido, comparação mais clara.

5.1.1 System Description

The linear system designed for simulation is the serial combination of two under damped modes, with distinct band pass behaviors.

One of the modes, henceforth termed as low-pass (lp) system, has time constant $\tau_{lp} = 1$ s, natural frequency $\omega_{n,lp} = 10$ Hz and a damping constant of $\zeta_{lp} = 0.1$. The frequency response is given by:

$$G_{lp}(s) = \frac{100}{s^2 + 2s + 100} \tag{5.1}$$

The second mode is a high-pass (hp) system, with a much lower time constant $\tau_{hp} = 0.01$ s, natural frequency $\omega_{n,hp} = 1000$ Hz, same damping constant of $\zeta_{hp} = 0.1$ and two zeros, one at the origin and another one at 0.001. The high-pass frequency response is given by:

$$G_{hp}(s) = \frac{s^2 - 0.001s}{s^2 + 200s + 10^6} \tag{5.2}$$

Figure 5.1 shows the bode diagrams of both systems separately.

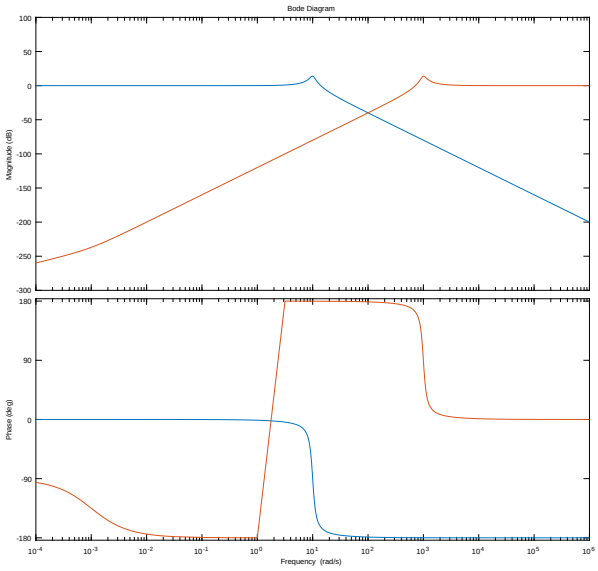

Figure 5.1: Bode diagram of both modes.

The resulting fourth order system is described as a state space representation, in a modal canonical form given by:

$$\begin{aligned} \dot{x}(t) &= Ax(t) + Bu(t) \\ y(t) &= Cx(t) + Du(t) \end{aligned} \tag{5.3}$$

where $x(t) \in \mathbf{R}^4$ is the state vector, $u(t) \in \mathbf{R}^1$ is the single input vector and $y(t) \in \mathbf{R}^1$ is the single output vector, and

$$A = \begin{bmatrix} -100 & 994.99 & 0 & 0 \\ -994.99 & -100 & 0 & 0 \\ 0 & 0 & -1 & 9.949 \\ 0 & 0 & -9.949 & -1 \end{bmatrix}$$

$$B = \begin{bmatrix} -24.6435 \\ -18.8943 \\ -4.1746 \\ -0.2675 \end{bmatrix} \tag{5.4}$$

$$C = \begin{bmatrix} 24.41 & -21.2522 & -0.1537 & 2.3977 \end{bmatrix}$$

$$D = 1$$

We simulate a pseudo-random binary sequence (PRBS) as input, with 200 samples and simulate the high-pass and low-pass systems separately according to Figure 5.2. As expected, the low-pass response is much slower. Just for comparison, if the same 200 samples of PRBS was generated over 20 seconds, the low-pass system response would account for more variations in the input. Figure 5.3 show the response of the final fourth order system.

The linear system is discretized using MATLAB's 'c2d'fic

The sampled-data observations are available according to:

$$y(t_k) = \mathbf{B}_d x(t) + \mathbf{D}_d u(t) + v(t_k) \tag{5.5}$$

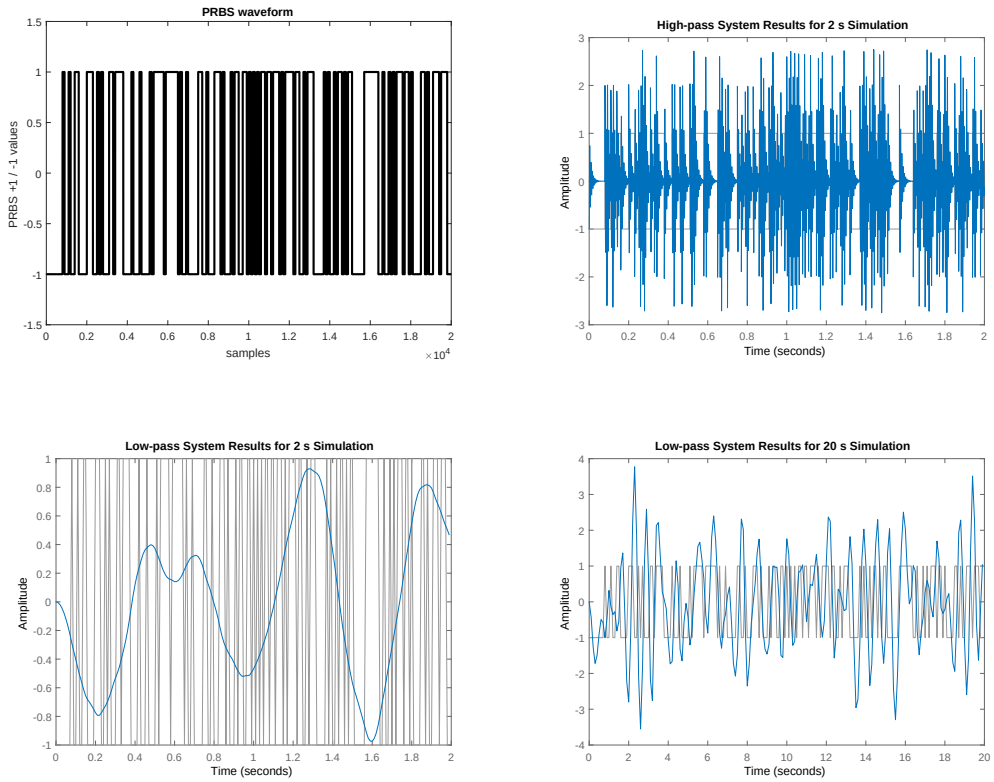

Figure 5.2: PRBS samples used as input; output of high-pass system, considering 2 seconds of simulation and low-pass system results for 2 and 20 seconds simulation

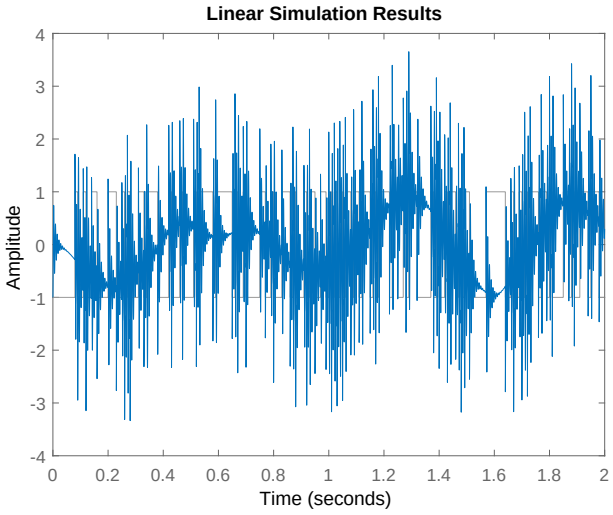

Figure 5.3: Output of the fourth order system to the PRBS input signal

where $v(t_k) \sim \mathcal{N}(0,R_{t_k})$ is the observation noise, with zero mean and covariance R_{t_k}. When time-stamp is not available, the observation vector is approximated by $\tilde{y}_i \approx y(t_k)$, where i is the index of the next time instant, multiple of T.

Discrete-time Kalman filter is used for estimation. Realizations of the estimated states and true values for both scenarios, with and without time-stamp, for a signal-to-noise ration in the observations of 40 dB are shown in Figures 5.4

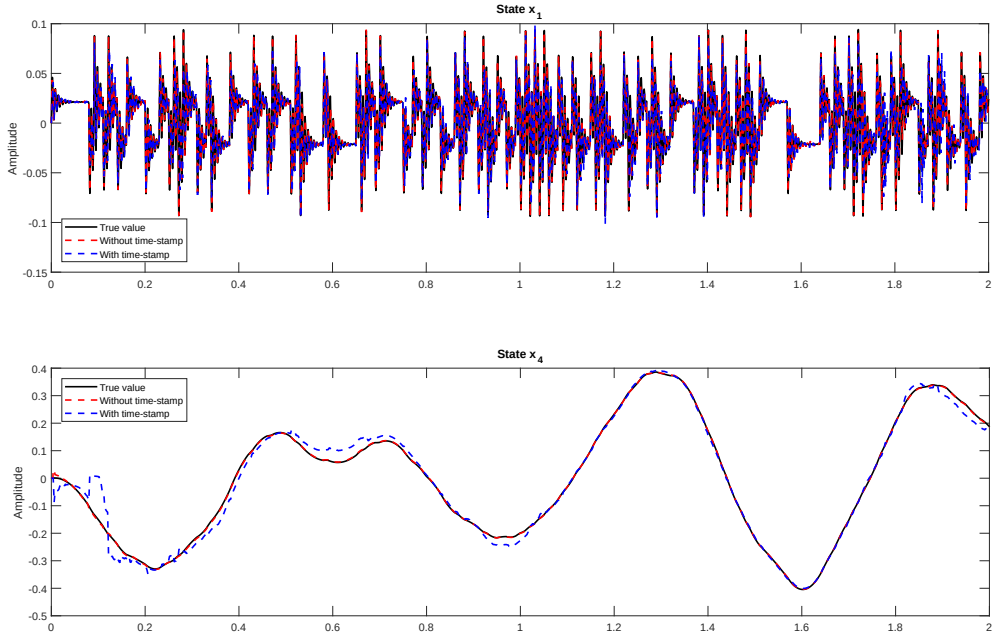

Figure 5.4: Estimated with time-stamp (red), without time-stamp (blue) and true (black) states x_1 and x_4.

Figure 5.5 presents a window data from 0 to 0.045 seconds of the first state RMSE for the algorithms with and without time-stamp. As expected, we observe a distancing from the RMSE at the instant the first observation was taken t_1, favoring the algorithm that considers time-stamp.

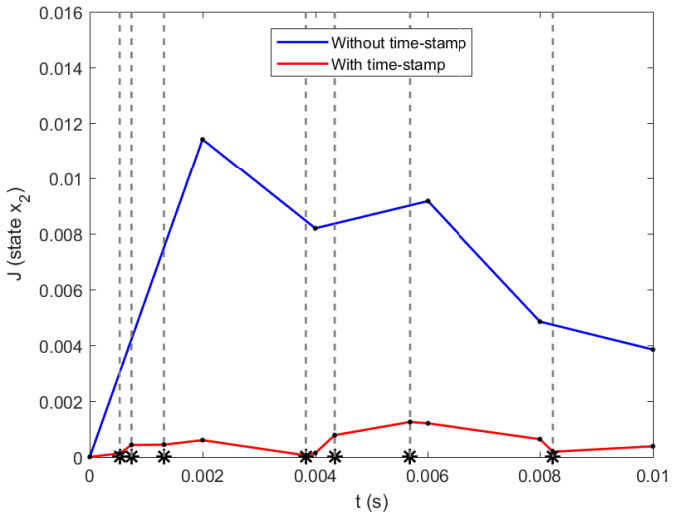

Figure 5.5: Temporal cut from 0.02 to 0.045 seconds, for a realization of pitch rate about the center of mass RMSE of both estimators, with (—) and without (—) time-stamp. Vertical dashed lines match the measurement sampling instants t_k. Black dots represent the regular estimation instants.

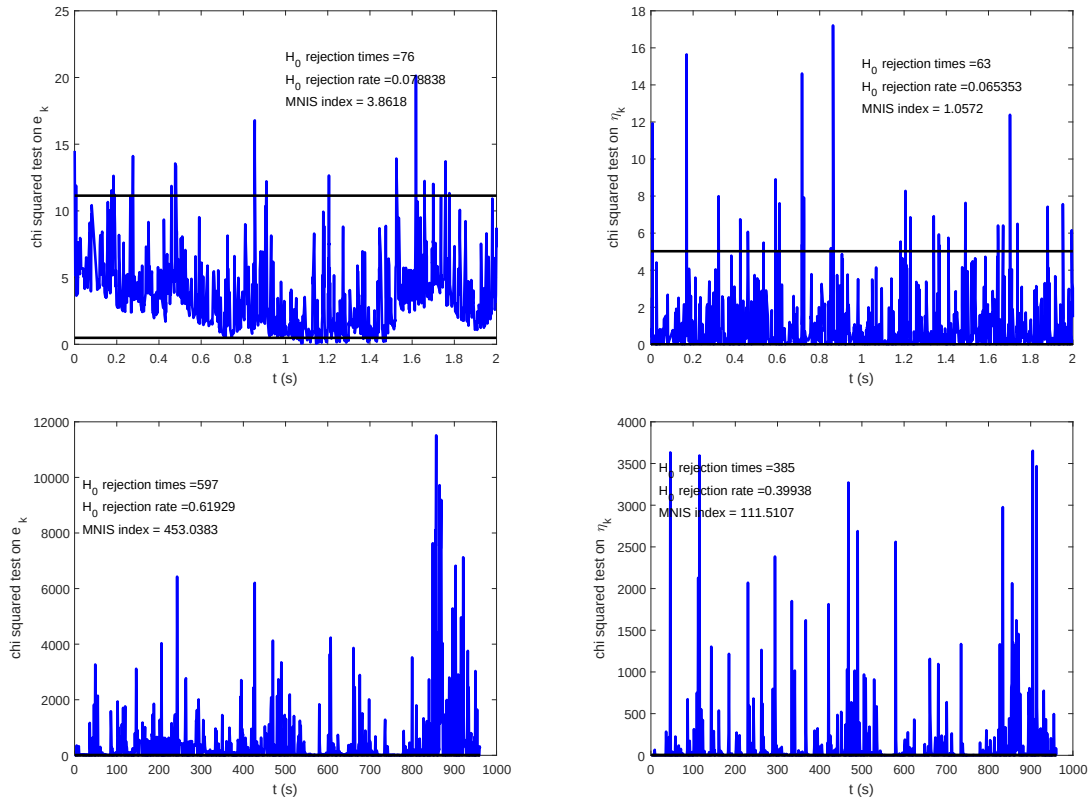

Figure 5.6: First group of subfigures.

5.1.2 Measurement Signal-to-Noise Ratio Variation

Changing input and measurement noise jointly

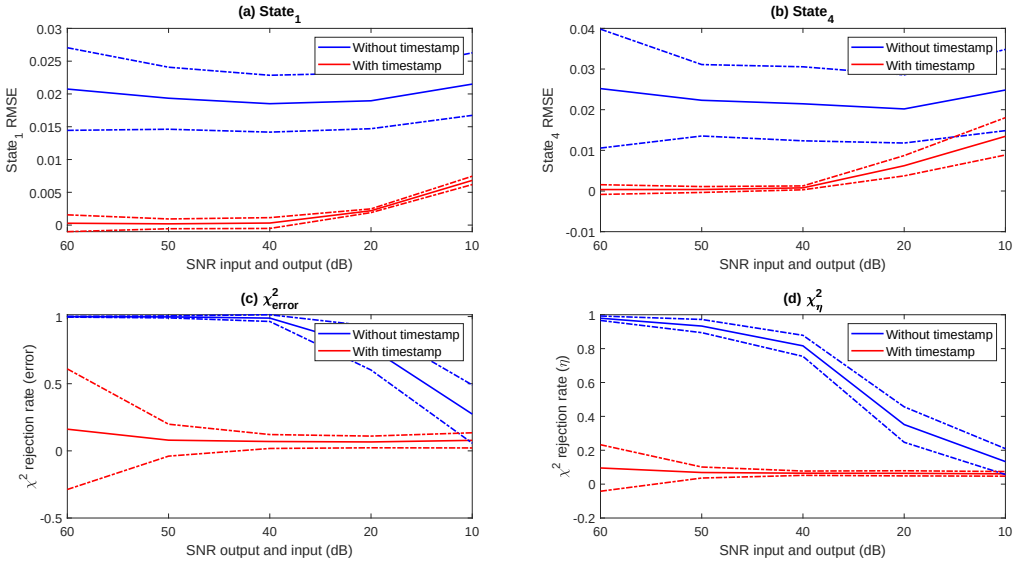

Figure 5.7: Performance, as a function of input and observation SNR

Changing only measurement noise

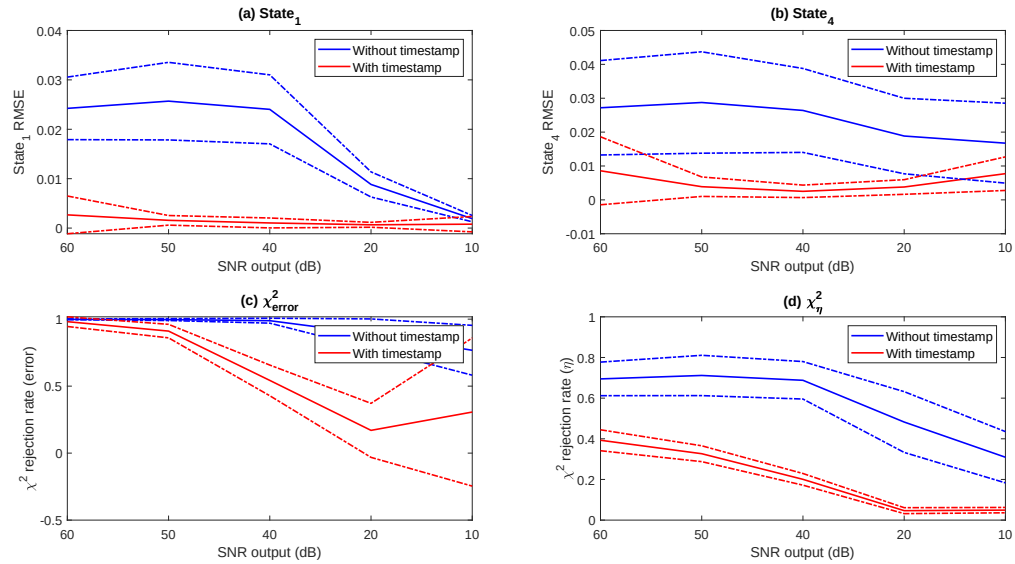

Figure 5.8: Performance, as a function of observation SNR

5.1.3 Average Sampling Rate Variation

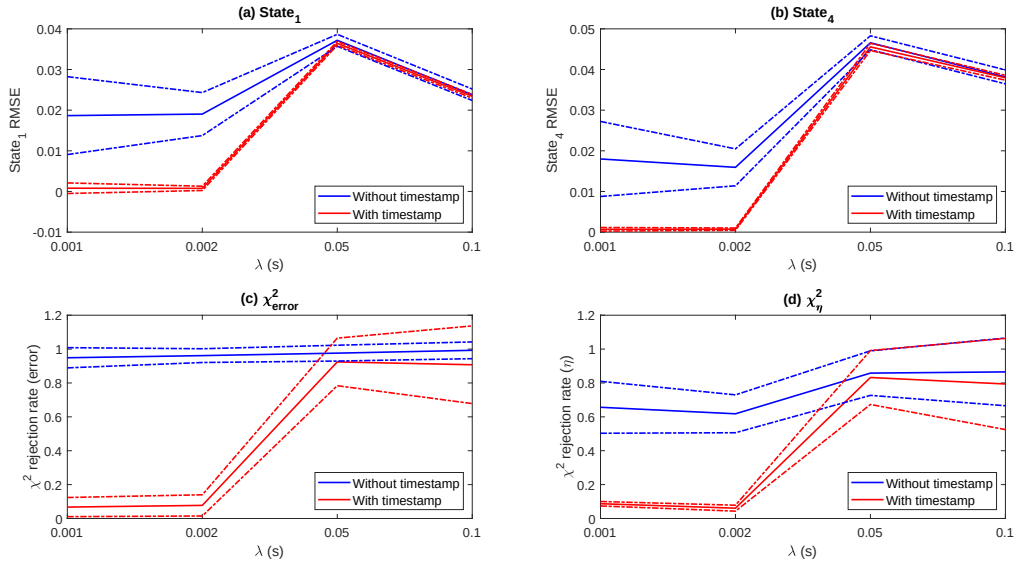

Figure 5.9: Performance, as a function of λ

5.1.4 Regular and Average Irregular Time Interval Relation Variation

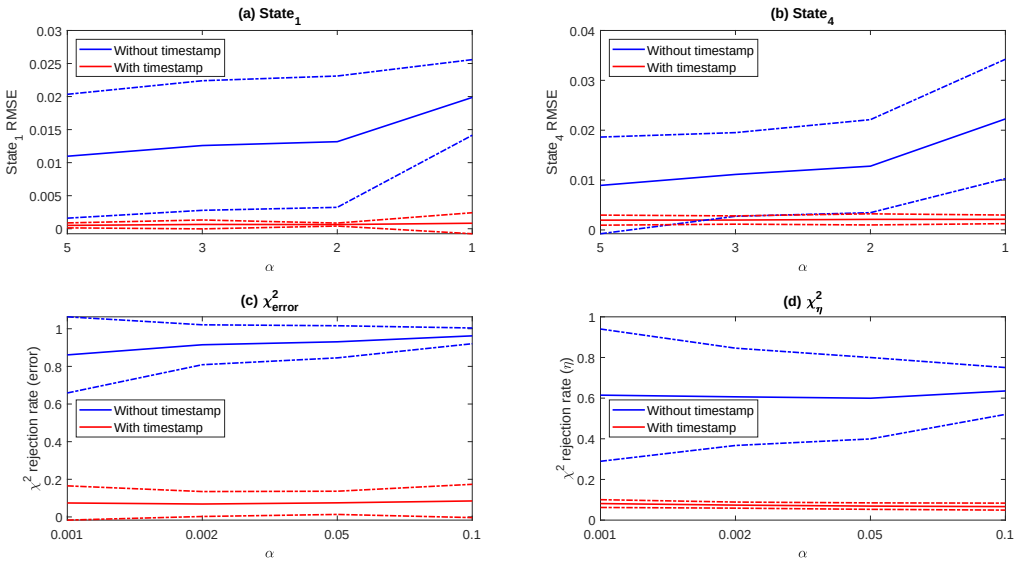

Figure 5.10: Performance, as a function of α

5.1.5 Average Time Delay

Ainda terá uma seção com a variação do time-delay e seu impacto no desempenho

5.2 Unicycle Position Estimation

Descrever as motivações por trás do estudo da amostragem irregular para problemas de rastreamento de robôs. Exemplos: medições feitas por câmeras não sincronizadas e utilizando redes de internet (com time delay).

5.2.1 System Description

Consider a nonholomonic moving robot, with the cinematic process model given by

$$\begin{aligned} \dot{p}_{\mathrm{x}} &= v\cos(\theta), \\ \dot{p}_{\mathrm{y}} &= v\sin(\theta), \\ \dot{\theta} &= u_1(t), \\ \dot{v} &= u_2(t), \end{aligned} \tag{5.6}$$

where p_{x} and p_{y} are the position coordinates, θ the angular orientation, v the linear velocity and inputs u_1 and u_2 are the angular velocity ω and the linear acceleration a, respectively. Figure 5.11 shows a schematic of the robot and its states,

The system described by 5.6 is discretized by a 4^{th} order Runge-Kutta method and the state vector x_i is given by $x_i \triangleq [p_{\mathrm{x},i}\ p_{\mathrm{y},i}\ \theta_i\ v_i]^T$.

The observation model $y(t_k) \in \mathbb{R}^2$

$$y(t_k) = \begin{bmatrix} p_{\mathrm{x}}(t_k) \\ p_{\mathrm{y}}(t_k) \end{bmatrix} + v(t_k), \tag{5.7}$$

is given by the position coordinates and $v(t_k) \sim \mathcal{N}(0, R_{t_k})$ is the observation noise, with zero mean and covariance R_{t_k}. When time-stamp is not available, the observation vector is approximated by $\tilde{y}_i \approx y(t_k)$, where i is the index of the next time instant, multiple of T.

Input vector $u_i = [\omega_i\ a_i]^T$ is measured by a girometer and accelerometer, respectively. We assume that

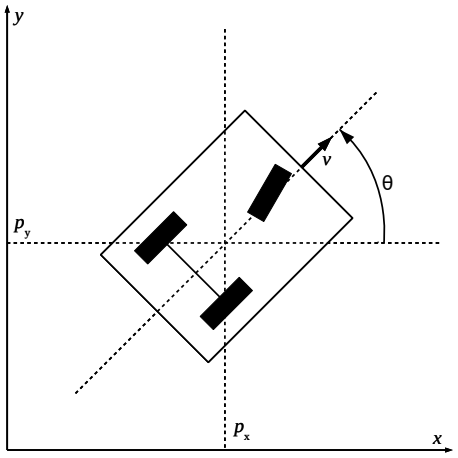

Figure 5.11: Nonholomonic robot system representation. The system states p_x, p_y, v and θ are highlighted.

$$u_i = \tilde{u}_i - w_i, \tag{5.8}$$

where $\tilde{u}$ is the sensors measured valueand $w \sim \mathcal{N}(0,Q_i)$ represents the corresponded noise, of zero mean and covariance Q_i.

We simulate 60 seconds of robot movement, considering a step size of $\delta t_{\text{sim}} = 10^{-4}$. Irregular sampling time intervals h_k are simulated by the exponential probability distribution function from MatLab™ and approximated to the nearest discrete time instant, from the 600,000 available samples. Input signals were generated arbitrarily according to Figure 5.12. Figure 5.13 shows robot trajectory on xy-plane for the given input signals, leaving from point (0,0), as well as a realization of noisy and aperiodic measurements with signal-to-noise ratio of $\text{SNR}_\text{y} = 30$ dB and $\lambda = 0.3$ s as red dots and the hatched blue line represents UKF estimation, considering time-stamp, $\alpha = 5$ and $\text{SNR}_\text{u} = 10$ dB.

To analyze the effect of considering time-stamp in the estimation algorithm, we use the performance index J

$$J = \frac{\sum_{i=1}^{N} \sqrt{(\hat{p}_{\text{x},i} - p_{\text{x},i})^2 + (\hat{p}_{\text{y},i} - p_{\text{y},i})^2}}{N} \tag{5.9}$$

where $\hat{p}_{\text{x},i}$ and $\hat{p}_{\text{y},i}$ are filter position estimates produced at a regular interval T, $\hat{p}_{\text{x},i}$ and $\hat{p}_{\text{y},i}$ the true coordinates of the robot at the same time instants and N the total number of estimates. This index represents the average estimator position error in xy-plane.

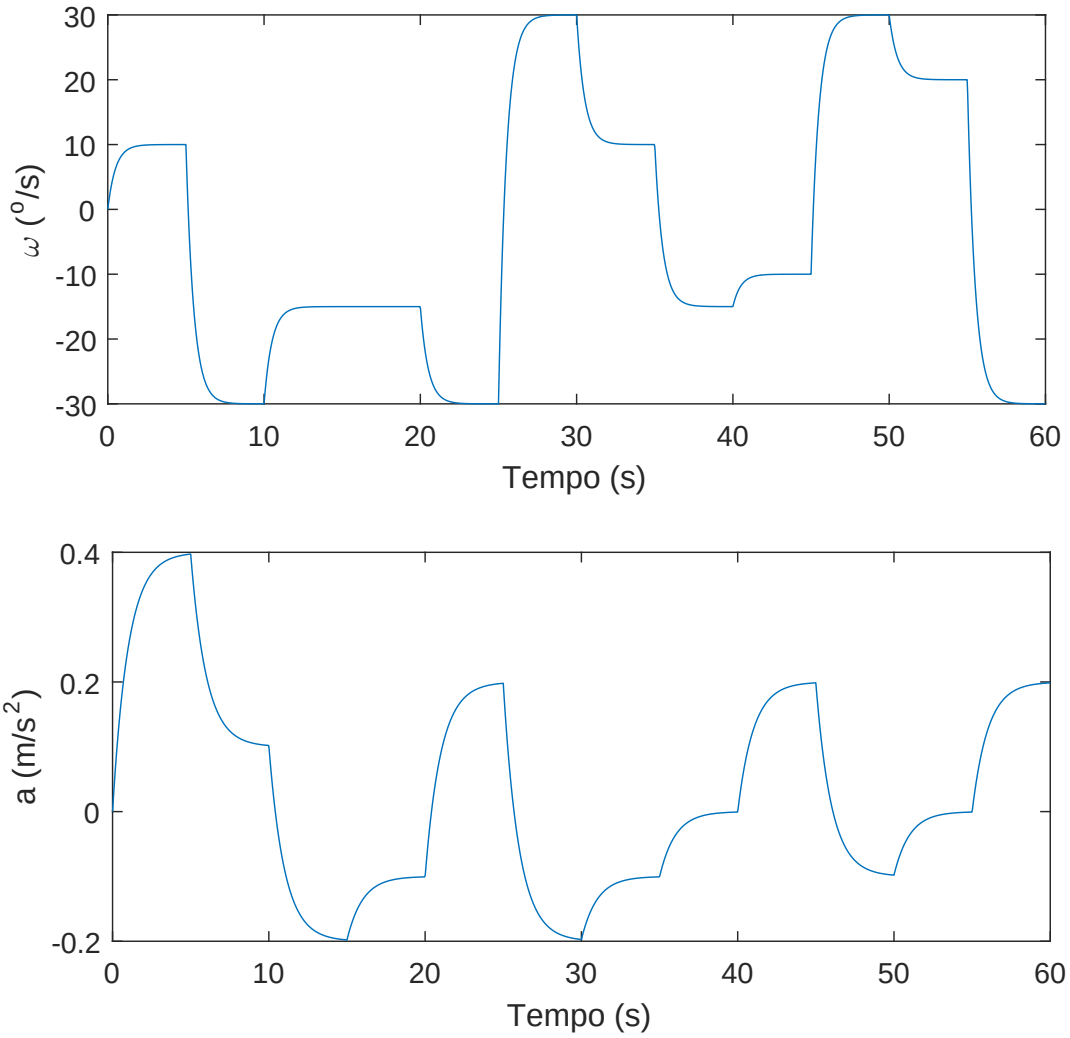

Figure 5.12: Simulation input signals. (a) shows temporal sequence of angular velocity ω and (b) shows linear acceleration a.

Figure 5.14 shows a timespan from 0 to 1.3 seconds of a J realization, considering $\lambda = 0.5$, $\alpha = 5$, $\text{SNR}_\text{y} = 60dB$ dB and $\text{SNR}_\text{u} = 20$ dB, for the UKF considering and not considering time-stamp. Black dots represent the regular time instants kT whereas the asterisks on x-axis match the exact measurement instants t_k. As expected, before the first data assimilation steps, both performances are identical. Since the first measurement t_1 was taken almost at the same time as regular estimation time instant $4T$, both estimation performances maintain close to each other. That is because the approximation error due to $\tilde{y}_i \approx y(t_k)$ is irrelevant. At t_2 we can observe significant deviation from index J in benefit of the algorithm considering time-stamp, since it performs data assimilation at

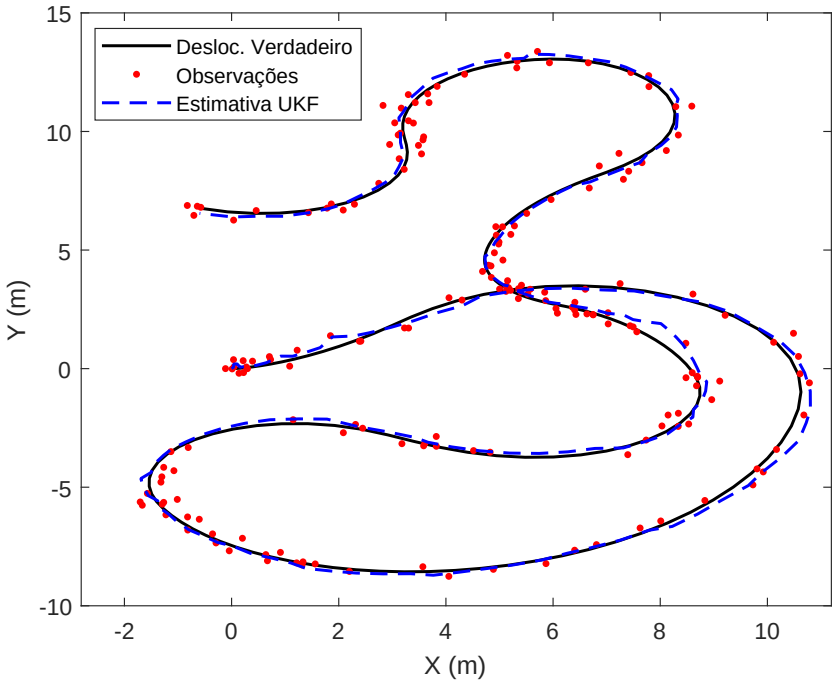

Figure 5.13: True position, noisy measurements and UKF estimates considering time-stamp, for a measurement noise of $\text{SNR}_y = 30$ dB, $\lambda = 0.3$ s and $\alpha = 5$.

the exact time measurement was taken. The same effect can be noted at t_4, after 1 second of simulation, when there is a significant different between time the measurement was taken and the next regular estimation instant.

5.2.2 Measurement Signal-to-Noise Ratio Variation

In this subsection we compare the estimation performance impact of considering time-stamp in the algorithm, by varying the measurement noise level. The signal-to-noise ratio for the input sensors and the measurement average time interval are held constant, $\text{SNR}_u = 20$ dB and $\lambda = 0.1$ s.

We considered an observation signal-to-noise variation of $\text{SNR}_y = \infty$, 80, 60, 40, 20, 10 dB. That is, initially the system was simulated considering no measurement noise and then it was gradually increased. For each noise scenario, we ran 100 realizations of the random variables for each algorithm and Figure 5.15 shows the results. Solid lines represent the average values for J and the dashed lines are the 95% confidence interval.

Falta incluir resultados com time-delay

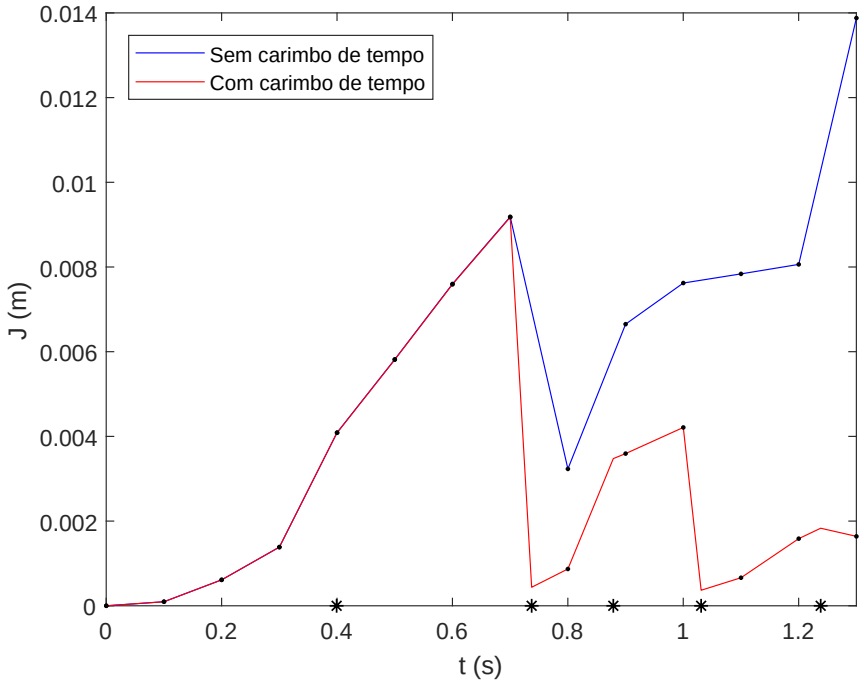

Figure 5.14: Temporal cut from 0 to 1.3 seconds, for a realization of J of both estimators, with and without time-stamp. Asterisks on x axis match the measurement sampling instants t_k. Black dots represent the regular estimation instants, same as input regular sampling instants.

É possível observar que o estimador que considera o carimbo de tempo possui desempenho estatisticamente superior apenas para baixos níveis de ruído da observação. Quando SNR_y *é igual a* ∞ *e* 80 *dB, o índice de desempenho* J *do filtro com carimbo de tempo é aproximadamente* 1.25 *e* 1.26 *cm, respectivamente, mais preciso do que sem carimbo de tempo e com variância pequena. Quando a relação sinal ruído se aproxima de* 40 *dB, no entanto, não é possível distinguir estatisticamente o efeito de se considerar ou não carimbo de tempo.*

5.2.3 Average Sampling Rate Variation

We now consider the variation of the average time interval that observations are taken, according to $\lambda = 0.1, 0.2, 0.3, 0.4, 0.5, 0.6$ s, maintaining the other parameters constant, namely the noise level of inputs and observations, $\text{SNR}_\text{u} = 20$ dB and $\text{SNR}_\text{y} = 40$ dB, respectively. We carried out 100 realizations for each λ and for each algorithm and Figure 5.16 presents the results. Again, the solid lines are the average values of J and the 95% confidence interval is between the dashed lines.

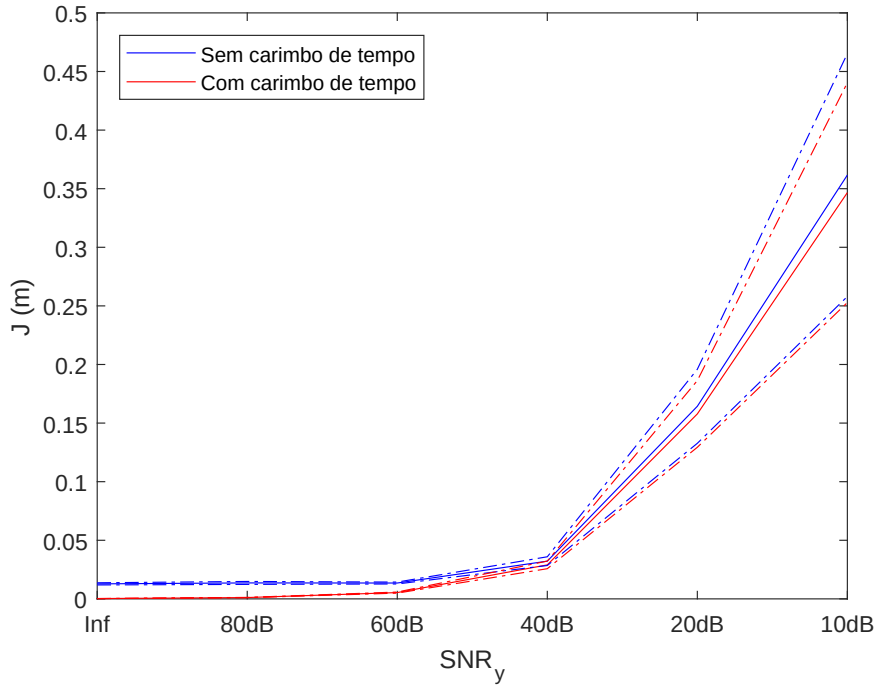

Figure 5.15: Performance index J variation, as a function of measurement noise for both UKF algorithms considering and not considering time-stamp

Os resultados obtidos demonstram que a diferença no desempenho dos filtros é mais significativa para intervalos de tempo mais espaçados, mantendo-se a dinâmica do sistema e os outros parâmetros fixos. Inicialmente, para valores pequenos de λ *, não há diferença estatística entre o desempenho dos estimadores, mas a medida que o intervalo cresce, ela aparece, chegando a aproximadamente* 3.1 *cm para um* $\lambda = 0.6$ *s. Uma interpretação possível é que, se o intervalo de tempo médio das observações for muito pequeno em comparação com a velocidade em que a dinâmica do sistema varia, o erro de aproximação do instante de amostragem das observações* t_k *é reduzido. O ruído do sensor pode acabar sendo mais relevante do que o erro devido ao tempo incorreto de assimilação.*

5.2.4 Regular and Average Irregular Time Interval Relation Variation

We also analyze the performance impact of varying the parameter α, which is the relation between regular input time interval T and average measurements time interval λ. The simulated values were $\alpha = 10, 5, 2, 1$. That means we start with higher frequency values for input sampling in comparison to measurement sampling and this values is

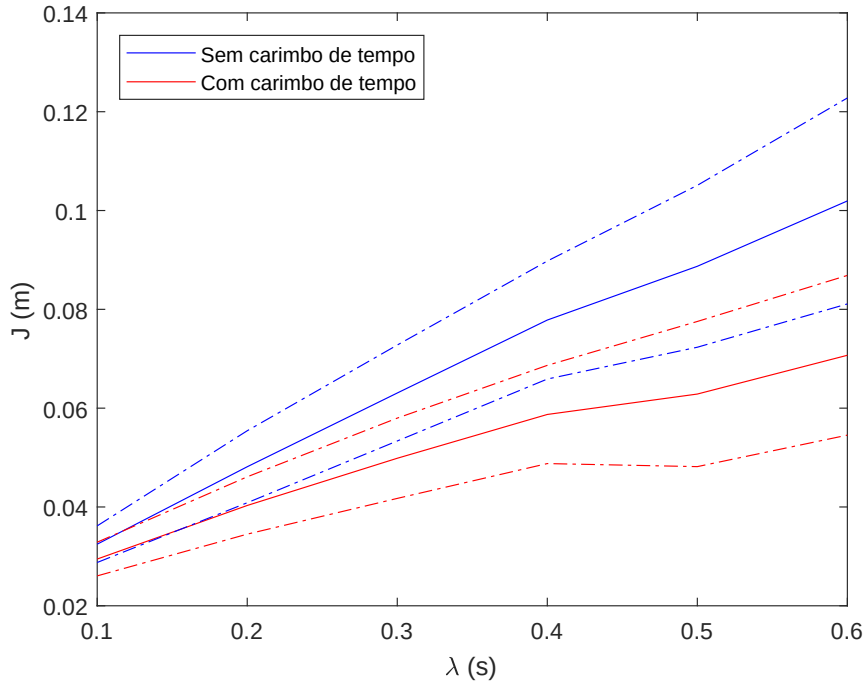

Figure 5.16: Performance index J variation, as a function of measurement noise both UKF algorithms considering and not considering time-stamp

gradually decreased. Other parameters were maintained constant $\text{SNR}_\text{u} = 20$ dB and $\text{SNR}_\text{y} = 40$ dB.

The same way we did for the other scenarios, 100 realizations were simulated and Figure 5.17 presents the results. Solid lines are the average values for J and dashed lines represent the 95% confidence interval.

Nota-se que, quando o carimbo de tempo é considerado, não há diferença significativa em se variar o α no desempenho do filtro, com o índice de desempenho J se mantendo pouco abaixo dos 3 cm. Ou seja, não importa a relação entre as frequências de amostragem da observação e das entradas. Por outro lado, quando não se considera o carimbo de tempo, essa relação se torna relevante para o índice de desempenho do estimador. Quanto mais lento a frequência da entrada em comparação com a frequência da saída, maior o erro obtido. Para o caso mais extremo utilizado, $\alpha = 1$, a diferença no índice J foi mais do que o dobro. Esse resultado era esperado, uma vez que quanto maior o valor de α, mais rápida é a taxa de discretização do modelo de processo em relação à frequência dos sensores de observação. Consequentemente, o erro obtido na aproximação $\tilde{y}(i) \approx y(t_k)$ diminui.

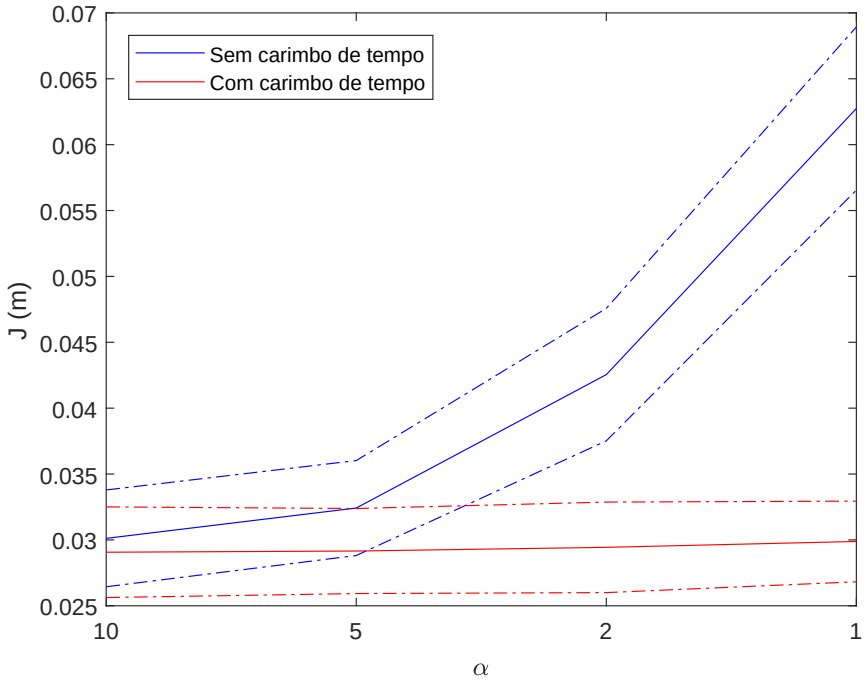

Figure 5.17: Performance index J variation, as a function of measurement noise both UKF algorithms considering and not considering time-stamp

5.2.5 Average Time Delay

Ainda terá uma seção com a variação do time-delay e seu impacto no desempenho

Chapter 6

Conclusions

6.1 Project Overview

Investigou-se isso e aquilo... (caso algum leitor pule direto para a conclusão)

6.2 Main Results

Como os resultados corroboram os objetivos perseguidos. O que é relevante dizer sobre cada objetivo descrito no capítulo 1, com o que foi feito no trabalho.

Autocrítica sobre o trabalho: alguma hipótese foi pouco realista? o que não foi feito tão bem? o que foi feito bem?

6.3 Future Work

Talvez uma lista itemizada Trabalhos futuros podem vir diretamente da autocrítica.

Bibliography

Anxi, Y., Diannong, L., Weidong, H., and Zhen, D. (2005). A unified out-of-sequence measurements filter. In *IEEE National Radar Conference - Proceedings*, pages 453–458.

Arulampalam, M. S., Maskell, S., Gordon, N., and Clapp, T. (2002). A Tutorial on Particle Filters for Online Nonlinear / Non-Gaussian Bayesian Tracking. *IEEE Transactions on Signal Processing*, 50(2):174–188.

Bar-Shalom, Y. (2000). Update with out-of-sequence measurements in tracking: Exact solution. *Proceedings of SPIE*, 4048(3):769–778.

Challa, S., Evans, R. J., and Wang, X. (2003). A Bayesian solution and its approximations to out-of-sequence measurement problems. *Information Fusion*, 4:185–199.

Chen, B., Yu, L., Zhang, W.-A., and Liu, A. (2013). Robust Information Fusion Estimator for Multiple Delay-Tolerant Sensors With Different Failure Rates. *IEEE Transactions on Circuits and Systems I: Regular Papers*, 60(2):401–414.

Dasarathy, B. (2001). Information Fusion - what, where, why, when, and how? *Information Fusion*, 2(2):75–76.

Elmenreich, W. (2002). An introduction to sensor fusion. Research report, Vienna University of Technology.

Eng, F. and Gustafsson, F. (2005). SYSTEM IDENTIFICATION USING MEASUREMENTS SUBJECT TO STOCHASTIC TIME JITTER. *IFAC Proceedings Volumes*, 38:1179–1184.

Fatehi, A. and Huang, B. (2017). Kalman filtering approach to multi-rate information fusion in the presence of irregular sampling rate and variable measurement delay. *Journal of Process Control*, 53:15–25.

Fridman, E. (2014). Introduction to time-delay and sampled-data systems. In *2014 European Control Conference (ECC)*, pages 1428–1433. IEEE.

Gopalakrishnan, A., Kaisare, N. S., and Narasimhan, S. (2010). Incorporating delayed and infrequent measurements in Extended Kalman Filter based nonlinear state estimation. *Journal of Process Control*, 21:119–129.

Hadidi, M. and Schwartz, S. (1979). Linear recursive state estimators under uncertain observations. *IEEE Transactions on Automatic Control*, 24(6):944–948.

Han, C. and Zhang, H. (2009). Linear optimal filtering for discrete-time systems with random jump delays. *Signal Processing*, 89(6):1121–1128.

Hu, R. J., Wang, Z., Alsaadi, F. E., and Hayat, T. (2017). Event-based filtering for time-varying nonlinear systems subject to multiple missing measurements with uncertain missing probabilities. *Information Fusion*, 38:74–83.

Hyberts, S. G., Robson, S. A., and Wagner, G. (2013). Exploring signal-to-noise ratio and sensitivity in non-uniformly sampled multi-dimensional NMR spectra. *Journal of Biomolecular NMR*, pages 167–178.

Jaffer, A. G. and Gupta, S. C. (1971). Recursive Bayesian Estimation With Uncertain Observation. *IEEE Transactions on Information Theory*, I(September):614–616.

Julier, S. J. and Uhlmann, J. K. (2004). Unscented Filtering and Nonlinear Estimation. *Proceedings of the IEEE*, 92(3):401–422.

Kanchanaharuthai, A. and Wongsaisuwan, M. (2002). Stochastic H/sub 2/-optimal controller design for sampled-data systems with random sampled measurement. In *Proceedings of the 41st SICE Annual Conference. SICE 2002.*, volume 3, pages 2042–2047. Soc. Instrument & Control Eng. (SICE).

Khaleghi, B., Khamis, A., Karray, F. O., and Razavi, S. N. (2013). Multisensor data fusion: A review of the state-of-the-art. *Information Fusion*, 14(1):28–44.

Kunoh, F. M. (2015). *Procedimento para Detecção de Falseamento via Amostragem Não Uniforme*. PhD thesis, Universidade Federal de Minas Gerais.

Lin, H. and Sun, S. (2016). Distributed fusion estimator for multi-sensor asynchronous sampling systems with missing measurements. *IET Signal Processing*, 10(7):724–731.

Liu, Q., Wang, Z., He, X., and Zhou, D. H. (2014). A survey of event-based strategies on control and estimation. *Systems Science and Control Engineering*, 2(1):90–97.

Lu, X., Zhang, H., Wang, W., and Teo, K. L. (2005). Kalman filtering for multiple time-delay systems. *Automatica*, 41(8):1455–1461.

Ma, J. and Sun, S. (2011). Optimal Linear Estimators for Systems With Random Sensor Delays , Multiple Packet Dropouts and Uncertain Observations. *IEE TRANSACTIONS ON SIGNAL PROCESSING*, 59(11):5181–5192.

Marvasti, F. (2001). *Nonuniform Sampling Theory and Practice*. Springer US, 1 edition.

Micheli, M. and Jordan, M. I. (2002). Random sampling of a continuous-time stochastic dynamical system. In *in Proc. of the 15th International Symposium on the Mathematical Theory of Networks and Systems (MTNS 2002), (University of Notre Dame, South)*.

Middleton, D. and Esposito, R. (1968). Simultaneous Optimum Detection and Estimation of Signals in Noise. *IEEE Transactions on Information Theory*, 14(3):434–444.

Miskowicz, M. (2006). Send-on-delta concept: An event-based data reporting strategy. *Sensors*, 6(1):49–63.

Moayedi, M., Foo, Y. K., and Soh, Y. C. (2011). Filtering for networked control systems with single/multiple measurement packets subject to multiple-step measurement delays and multiple packet dropouts. *International Journal of Systems Science*, 42(3):335–348.

Nahi, N. (1969). Optimal recursive estimation with uncertain observation. *IEEE Transactions on Information Theory*, 15(4):457–462.

Peñarrocha, I., Sanchis, R., and Romero, J. A. (2012). State estimator for multisensor systems with irregular sampling and time-varying delays. *International Journal of Systems Science*, 43(8):1441–1453.

Phillips, C. L. and Nagle, H. T. (1995). *Digital control system analysis and design*. Prentice-Hall, Inc.

Richard, J.-P. (2003). Time-delay systems: an overview of some recent advances and open problems. *Automatica*, 39(10):1667–1694.

Sahebsara, M., Chen, T., and Shah, S. L. (2007). Optimal filtering with random sensor delay, multiple packet dropout and uncertain observations. *International Journal of Control*, 80(2):292–301.

Schenato, L., Sinopoli, B., Franceschetti, M., Poolla, K., and Sastry, S. S. (2007). Foundations of Control and Estimation Over Lossy Networks. *Proceedings of the IEEE*, 95(1):163–187.

Shen, B., Wang, Z., and Huang, T. (2016). Stabilization for sampled-data systems under noisy sampling interval. *Automatica*, 63:162–166.

Shuli Sun, Lihua Xie, Wendong Xiao, and Nan Xiao (2008). Optimal Filtering for Systems With Multiple Packet Dropouts. *IEEE Transactions on Circuits and Systems II: Express Briefs*, 55(7):695–699.

Sinopoli, B., Schenato, L., Franceschetti, M., Poolla, K., Jordan, M. I., and Sastry, S. S. (2004). Kalman filtering with intermittent observations. *IEEE Transactions on Automatic Control*, 49(9):1453–1464.

Sivrikaya, F. and Yener, B. (2004). Time Synchronization in Sensor Networks: A Survey. *IEEE Network*, 18(4):45 – 50.

Tabuada, P. (2007). Event-Triggered Real-Time Scheduling of Stabilizing Control Tasks. *IEEE Transactions on Automatic Control*, 52(9):1680–1685.

Wang, Z., Ho, D. W., Liu, Y., and Liu, X. (2009). Robust H_∞ control for a class of nonlinear discrete time-delay stochastic systems with missing measurements. *Automatica*, 45(3):684–691.

Westenberger, A., Waldele, S., Dora, B., Duraisamy, B., Muntzinger, M., and Dietmayer, K. (2013). Multi-sensor fusion with out-of-sequence measurements for vehicle environment perception. In *Proceedings - IEEE International Conference on Robotics and Automation*.

Willner, D., Chang, C. B., and Dunn, K. P. (1976). Kalman filter algorithms for a multisensor system. In *IEEE Conference on Decision and Control including the 15th Symposium on Adaptive Processes*, volume 15, pages 570–574.

Yan, B., Lev-Ari, H., and Stankovic, A. M. (2017). Networked State Estimation with Delayed and Irregularly-Spaced Time-Stamped Observations. *IEEE Transactions on Control of Network Systems*, 5870(c):1–1.

Yan, L., Xiao, B., Xia, Y., and Fu, M. (2010). State estimation for asynchronous multirate multisensor nonlinear dynamic systems with missing measurements. *IET Signal Proces*, 4(6):728–739.

Zhu, C., Xia, Y., Xie, L., and Yan, L. (2013). Optimal linear estimation for systems with transmission delays and packet dropouts. *IET Signal Processing*, 7(9):814–823.

Zou, L., Wang, Z.-D., and Zhou, D.-H. (2017). Event-based Control and Filtering of Networked Systems: A Survey. *International Journal of Automation and Computing*, 14(3):239–253.